JM PAPERS

Effect of electrostatic forces on the dispersion of like-charged solid particles transported by homogeneous isotropic turbulence

Athanasios Boutsikakis[1], Pascal Fede[1],† and Olivier Simonin[1]

[1]Institut de Mécanique des Fluides de Toulouse (IMFT), Université de Toulouse, CNRS, 31400 Toulouse, France

The effect of electrostatic forces on the dispersion of small like-charged inertial particles transported by a homogeneous isotropic turbulent flow is analysed by means of direct numerical simulations coupled with the Lagrangian tracking of charged particles. The results show that particle dispersion decreases for increasing charge. Since turbulent particle dispersion is related to the intensity of particle agitation and to the Lagrangian particle integral time scale, we analyse the effects of electrostatic forces on these two quantities. Particle agitation decreases for increasing particle charge. In fact, particle kinetic energy is not directly modified by electrostatic forces, which are conservative, it is rather the particle entrainment by fluid turbulence that is modified. To support this claim, one shows that the fluid–particle velocity covariance is destructed by electrostatic forces, a destruction can be predicted by drawing an analogy between inter-particle collisions and Coulomb collisions. As expected, electrostatic forces decorrelate particle velocities leading to a decrease of the Lagrangian particle integral time scale. Finally, one shows that the analogy with inter-particle collisions allows us to predict the reduction of particle dispersion.

Key words: particle/fluid flow

1. Introduction

Particle-laden turbulent flows are encountered in many practical applications as in geophysical flows with the dispersion of volcanic ashes, sediment transport or the formation of dunes; in engineering processes with a pulverized coal furnace, pneumatic powder conveying; or in health/medicine with drugs dispersion in the respiratory tract, or the dispersion of a virus by coughing. In all of these examples the physics controlling

† Email address for correspondence: pascal.fede@imft.fr

the particle dispersion is complex because of the multi-physics nature of particle-laden flows. As a non-exhaustive list, one can mention particle-turbulence interaction, turbulence modulation, inter-particle collisions, particle bouncing on smooth or rough walls and inter-particle electrostatic forces. Although it has been neglected over a long time, the effect of the particle charges on the flow dynamics may be very important. As, for example, in electrostatic precipitators, where the granular phase is diluted, particles are charged and an electric field is used to remove the particles from the gas (Parker 1997). Also, as denoted by Pruppacher & Klett (2010), the charges may also have an effect on the coalescence kernel of rain droplets.

This paper focuses on the dispersion of charged solid particles transported by a turbulent gas flow. More precisely, we investigate the self-particle turbulent dispersion (Monin & Yaglom 2007) which is characterized by the mean square particle displacement. The particulate flow is very diluted allowing us to neglect turbulence modulation by the particles as well as inter-particle collisions. In such a framework, Li & Ahmadi (1993) investigated the effect of electric charges on the deposition of particles on a flat vertical charged wall. As expected, the authors showed that the electric field leads to an increase of the deposition velocity and the smaller the particle response, the largest is this increase. It is well known that inertial particles suspended in a turbulent fluid flow may concentrate in preferential regions of the turbulence (Fessler, Kulick & Eaton 1994). This phenomenon, called preferential concentration or clustering, results from the competition between the drag and centrifugal forces. In 2010 Lu *et al.* (2010*a*) analysed experiments to understand how the clustering of solid charged inertial particles is modified by the charges. They show that when particles have the same charge, the Coulomb repulsion force leads to a decrease of the clustering under a given length scale. Theoretical descriptions have also been made to predict the effect of electric charges on the clustering of particles. Alipchenkov, Zaichik & Petrov (2004) for non-settling, and Lu, Nordsiek & Shaw (2010*b*) for settling particles in a homogeneous isotropic turbulence derived a theoretical expression for the radial distribution function. Particularly, Lu *et al.* (2010*b*) validate their model by comparison with experimental measurements obtained for particles having a small Stokes number. The investigation on larger Stokes numbers is generally accomplished by means of numerical simulation. However, as clearly shown by Yao & Capecelatro (2018) and Boutsikakis *et al.* (2020), the way to compute accurately the electrostatic forces in an unbounded domain can be tricky and/or inaccurate. Despite these difficulties, interesting information has been obtained from numerical simulations. As, for example, Lu & Shaw (2015) show how the charges modify the collision kernel and especially how they affect the inter-particle relative velocity. In a more complex geometry, namely a turbulent duct, Grosshans *et al.* (2021) showed that the charges also affect particle motion at a large scale.

All of these works mainly scrutinized how the electric charges modify the spatial distribution of the particles. However, at first order one can wonder what such an effect would be on particle dispersion. Karnik & Shrimpton (2012) slightly addressed this question by showing that the mean variance of particle displacement decreases with increasing particle charges. Boutsikakis *et al.* (2020) found similar results and showed that particle agitation intensity decreases for increasing charges. In fact, particle dispersion has two main ingredients: first the particle agitation and second the Lagrangian particle integral time scale. In the present paper, these two contributions are analysed in terms of an electrostatic Stokes number. We show how it is possible to predict the dispersion of like-charged particles by making an analogy between the inter-particle collisions and the Coulomb collisions (i.e. the effect of the electrostatic forces).

The paper is organized as following. The next section gives an overview of the numerical simulations in terms of a direct numerical simulation (DNS) solver and Lagrangian

particle tracking. The definitions and the relevance of the characteristic time scales are also discussed. Section 3 is dedicated to the modification of the dispersion coefficient by inter-particle electrostatic forces in terms of dynamic and electrostatic Stokes numbers. Then the analysis is split in two parts: first the modification of particle agitation (§ 4) and then the effect of electrostatic forces on the particle velocity auto-correlation (§5). The conclusions of this work are drawn in the last section.

2. Numerical simulation details

2.1. *Direct numerical simulation*

Direct numerical simulation of incompressible Navier–Stokes equations has been performed on a cubic domain of length L_b with full three-dimensional periodic boundary conditions. The numerical technique consists of a pseudo-spectral method where aliasing control was ensured by spherical truncation. In order to get a statistically stationary turbulence, the stochastic forcing proposed by Eswaran & Pope (1988) has been used. Such a spectral forcing scheme consists in forcing a given range of wavenumbers by a stochastic force based on a Wiener process. The range of the forced wavenumbers, that control the Eulerian integral length scale of the turbulence, L_f, has been chosen in order to limit the length of the largest eddies to $1/10$ of the domain size. For the variance and the time scale of the Wiener process, we followed the same methodology as Février, Simonin & Squires (2005) and Fede & Simonin (2006), where they adjust the forcing parameters so that the eddy lifetime turnover time scale $T_e = L_f/\sqrt{2q_f^2/3}$ is equal to the Eulerian integral time scale of the turbulence $\tau_E = \int_0^{+\infty} R_E(\tau)\,\mathrm{d}\tau$. The fluid velocity auto-correlation Eulerian function, $R_E(\tau)$, is obtained on motionless particles with

$$R_E(\tau) = \frac{\langle \boldsymbol{u}_f'(t, \boldsymbol{x}_E)\boldsymbol{u}_f'(t+\tau, \boldsymbol{x}_E)\rangle_p}{2q_f^2}, \tag{2.1}$$

where $\boldsymbol{u}_f'$ is the fluctuating fluid velocity, $q_f^2 = 1/2\langle \boldsymbol{u}_f'\boldsymbol{u}_f'\rangle_p$ the fluid kinetic energy (per unit mass) and $\langle . \rangle_p$ the average operator over the particles, here the motionless particles. In (2.1), $\boldsymbol{x}_E$ is the position of the motionless particles that have been randomly distributed within the domain. Similarly, one can define the Lagrangian fluid velocity auto-correlation function, $R_f(\tau)$, as

$$R_f(\tau) = \frac{\langle \boldsymbol{u}_f'(t, \boldsymbol{x}_f)\boldsymbol{u}_f'(t+\tau, \boldsymbol{x}_f)\rangle_p}{2q_f^2}. \tag{2.2}$$

Here, $\boldsymbol{x}_f$ is the position vector of fluid elements tracked during the numerical simulation. From the Lagrangian fluid velocity auto-correlation function, one obtains the Lagrangian fluid integral time scale by $\tau_f^t = \int_0^{+\infty} R_f(\tau)\,\mathrm{d}\tau$.

Table 1 gathers the relevant parameters and statistics of the turbulent fluid flow (time-averaged statistics have been performed over $\sim 45T_e$). The Kolmogorov length scale is given by $\eta_K = (\nu_f/\varepsilon)^{1/4}$, with ε being the dissipation rate measured in DNS, and the Kolmogorov time scale by $\tau_K = (\nu_f/\varepsilon)^{1/2}$. Direct numerical simulations have been performed with 256^3 grid points leading to a good resolution of the smallest turbulent scales, as $\eta_K \kappa_{max} \approx 3$ (with κ_{max} being the highest resolved wavenumber).

Parameters	Symbol	Value	Units
Computational domain length	L_b	2π	m
Fluid kinematic viscosity	ν_f	10^{-3}	$m^2\,s^{-1}$
Fluid density	ρ_f	1.0	$kg\,m^{-3}$
Fluid kinetic energy	q_f^2	3.16×10^{-2}	$m^2\,s^{-2}$
Eddy turn-over lifetime	T_e	4.49	s
Fluid longitudinal integral length scale	L_f/L_b	1.04×10^{-1}	—
Fluid integral time scale	τ_f^t/T_e	6.97×10^{-1}	—
Turbulent Reynolds number	Re_{L_f}	99.39	—
Kolmogorov length scale	η_K/L_f	3.50×10^{-2}	—
Kolmogorov time scale	τ_K/T_e	1.16×10^{-1}	—
Resolution	$\eta_K \kappa_{max}$	2.92	—

Table 1. Properties of the fluid and of the examined HIT.

2.2. *Discrete particle simulation*

For the particulate phase, we consider a disperse phase composed of N_p solid, spherical and charged particles. The motion of particles suspended in turbulent flows received much attention (Gatignol 1983; Maxey & Riley 1983). In the present case, on one hand, the particle density, ρ_p, is large compared with that of the fluid, and on the other hand the particle diameter, d_p, is small compared with the Kolmogorov length scale. Therefore, one can reasonably reduce the forces acting on the particle only to the drag force, $\boldsymbol{F}_d$, and the electrostatic force, $\boldsymbol{F}_e$. In such a framework, the single particle motion governing equations read as

$$\frac{\mathrm{d}\boldsymbol{x}_p}{\mathrm{d}t} = \boldsymbol{u}_p, \tag{2.3}$$

$$\frac{\mathrm{d}\boldsymbol{u}_p}{\mathrm{d}t} = \frac{\boldsymbol{F}_d}{m_p} + \frac{\boldsymbol{F}_e}{m_p}. \tag{2.4}$$

Introducing τ_p, which is the particle response time, the drag force reads as

$$\frac{\boldsymbol{F}_d}{m_p} = -\frac{f}{\tau_p}(\boldsymbol{u}_p - \boldsymbol{u}_{f@p}), \tag{2.5}$$

with $\tau_p = \rho_p d_p^2/(18\mu_f)$ and $f = 1 + 0.15Re_p^{0.687}$ (Schiller & Naumann 1935). The particle Reynolds number reads as $Re_p = d_p||\boldsymbol{u}_p - \boldsymbol{u}_{f@p}||/\nu_f$ and $\boldsymbol{u}_{f@p}$ is the instantaneous fluid velocity at the particle position undisturbed by the presence of the particle. Since the particle mass fraction is very low, the modulation of the turbulence by the particles (two-way coupling effect) is neglected. Consequently, the fluid velocity seen by the particles is directly computed by a third-order Lagrange polynomial interpolation scheme. For the analysis, one introduces the particle relaxation time scale, τ_{fp}^F, defined as $\tau_{fp}^F = \langle f/\tau_p \rangle_p^{-1}$.

For two charged particles p and q, the electrostatic force that acts on particle p due to particle q is given by the Coulomb law

$$\boldsymbol{F}_{e,q\to p} = \lambda \frac{Q_p Q_q}{||\boldsymbol{r}_{pq}||^3}\boldsymbol{r}_{pq}, \tag{2.6}$$

where $\lambda = 1/(4\pi\epsilon_0)$, with ϵ_0 the vacuum permittivity, Q_p and Q_q the electric charge of the p and q particle. In (2.6), $\boldsymbol{r}_{pq} = \boldsymbol{x}_p - \boldsymbol{x}_q$ is the distance vector between the two particles pointing to p. Hence, for a system of N_p like-charged particles, each particle interacts with the other $N_p - 1$ particles, so that the total electrostatic force is $\boldsymbol{F}_e = \sum_{q=1, q \neq p}^{N_p} \boldsymbol{F}_{e, q \rightarrow p}$. For details of the numerical method, we refer the reader to Boutsikakis *et al.* (2020).

2.3. *Characteristic time scales and Stokes numbers*

In order to compare the effect of electrostatic forces to the entrainment by turbulence, it is important to define a characteristic electrostatic time scale. To characterize the competition between the entrainment by turbulence and the electrostatic force, Alipchenkov *et al.* (2004) introduced the Coulomb number defined as $Ct = E_{el}/E_{turb}$. On one hand, as explained by Lu *et al.* (2010*a*), $E_{el} = \lambda Q_p^2/(m_p \eta_K)$ is the potential energy due to Coulomb interaction at dissipation scales (namely the Kolmogorov length scale, η_K). On the other hand, $E_{turb} = v_K^2$ is the 'kinetic energy of involvement of particles into small-scale turbulent motion'. Two main drawbacks arise when using such a Coulomb number. First, by definition it concerns only particles interacting with turbulence at the dissipation scale, hence having a small particle response time. Second and more important, such a Coulomb number does not take into account the particle density number. Hence, the analysis based on such a dimensionless number can not be extended to a case with a different number of particles. This last limitation has been overcome by Karnik & Shrimpton (2012) by introducing the electric settling velocity $v_{el} = \tau_p E_{rms} Q_p/m_p$. Indeed, as E_{rms} is the root-mean-square magnitude of the electric field, it is clearly a function of the particle number density. However, the level of E_{rms} results from the interactions of particles with turbulence, which can not be known *a priori*. Karnik & Shrimpton (2012) and later Yao & Capecelatro (2018) compare the electrostatic forces to the entrainment by turbulence with the dimensionless number $v_{el}/\sqrt{2q_f^2/3}$. From the particle motion equation, Lu *et al.* (2010*a*) and later Lu & Shaw (2015) define the electric settling velocity as the terminal velocity of two particles separated by a distance of the Kolmogorov length scale. The electric settling velocity is then fully written in terms of particle parameters $v_{el} = 2\tau_p Q_p^2/(m_p \eta_K^2)$ and the Coulomb turbulence number becomes $Ct = v_{el}/v_K$ (where v_K is the Kolmogorov characteristic velocity). Thus, the electric terminal velocity includes two effects, namely the interaction of the particle with the turbulence and the electrostatic forces. Boutsikakis *et al.* (2020) proposed another time scale characterizing the electrostatic forces independently of the turbulence itself,

$$\tau_{el} = \frac{1}{Q_p} \sqrt{\frac{3}{2} \frac{m_p}{\lambda n_p}}, \tag{2.7}$$

with $n_p = N_p/L^3$ (where N_p is the number of particles) the particle number density. To derive this expression, the authors conducted firstly a dimensional analysis and secondly they performed numerical simulations of like-charged particles in a vacuum. In that case, the particle trajectories are only governed by electrostatic forces. The particle velocity auto-correlation time scale, τ_p^t, is hence only dependent to the electrostatic forces and as such, an excellent candidate for being the characteristic time scale of these forces. Such a time scale is defined as the Lagrangian particle integral time scale, $\tau_p^t = \int_0^{+\infty} R_p(\tau)\, d\tau$,
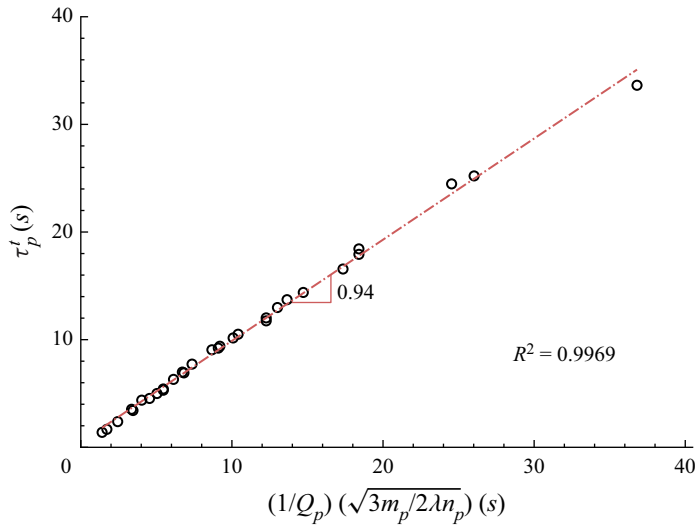
Figure 1. Comparison of particle velocity auto-correlation time scale measured in homogeneous isotropic dry granular flow of charged particles with the characteristic time scale of electrostatic forces proposed by Boutsikakis *et al.* (2020) and given by (2.7).

with the particle velocity auto-correlation function that reads as

$$R_p(\tau) = \frac{\langle \boldsymbol{u}'_p(t, \boldsymbol{x}_p) \boldsymbol{u}'_p(t + \tau, \boldsymbol{x}_p) \rangle_p}{2q_p^2}, \tag{2.8}$$

where $q_p^2 = 1/2 \langle \boldsymbol{u}'_{p,i} \boldsymbol{u}'_{p,i} \rangle_p$ is the so-called particle turbulent (or fluctuating) kinetic energy (per unit mass) which is also called the particle agitation in the paper. In figure 1 every marker corresponds to the measurement of τ_p^t coming from a different simulation with a different set of particle properties. All simulations concern like-charged particles of diameter $d_p = 5 \times 10^{-3}$ m in a tri-periodic computational domain of size L_b (see table 1). In order to perform the dimensional analysis, the following particle properties have been considered: $\rho_p = \{1.5, \mathbf{2.75}, 5, 10, 20\} \times 10^3$, $Q_p = \{2, 3, 4, \mathbf{5}, 6\} \times Q_0$, $N_p = \{1, 2.5, 5, \mathbf{10}, 25, 50, 100, 150\} \times 10^3$, where the values in bold correspond to the reference simulation and each other simulation entails only one parameter change. This figure shows the excellent agreement of the measured electrostatic time scale with the proposed characteristic time scale of electrostatic forces given by (2.7). One emphasizes that (2.7) differs slightly from the original expression proposed by Boutsikakis *et al.* (2020). The difference is only the coefficient $\sqrt{3/2}$ that we have introduced from correlation analysis on dry granular charged flows.

To better understand the competition between inter-particle electrostatic forces and particle-turbulence interaction, we defined several dimensionless numbers (i.e. several Stokes numbers) based on previous time scales. Firstly, for the dynamics of the particles, one can introduce the standard (dynamic) Stokes number defined as the ratio between the particle relaxation time scale τ_{fp}^F to the Lagrangian fluid integral time scale seen by inertial particles, $\tau_{f@p}^t$ (Deutsch & Simonin 1991). This last time scale is defined by $\tau_{f@p}^t = \int_0^{+\infty} R_{f@p}(\tau) \, \mathrm{d}\tau$ with the auto-correlation function of the fluid velocity seen by

938 A33-6

the particles that reads as

$$R_{f@p}(\tau) = \frac{\langle \boldsymbol{u}'_{f@p}(t, \boldsymbol{x}_p)\boldsymbol{u}'_{f@p}(t + \tau, \boldsymbol{x}_p)\rangle_p}{2q^2_{f@p}}. \tag{2.9}$$

In (2.9) the auto-correlation function is normalized by the fluid kinetic energy (per unit mass) seen by the particles which is given by $q^2_{f@p} = 1/2\langle \boldsymbol{u}'_{f@p}\boldsymbol{u}'_{f@p}\rangle_p$. To compare the electrostatic forces to the particle-turbulence interaction, we introduce the electrostatic Stokes number as τ^F_{fp}/τ_{el}. The asymptotic behaviour of the electrostatic Stokes number is obvious. Indeed, for $\tau^F_{fp}/\tau_{el} \rightarrow 0$, the inter-particle electrostatic forces are negligible, and the particle dispersion is controlled by the turbulence. In contrast, for $\tau^F_{fp}/\tau_{el} \rightarrow +\infty$, particle dynamics is controlled by electrostatic forces.

In the present numerical simulations, the particle diameter has been conserved constant, $d_p/\eta_K = 0.2$, and the particle density varies in order to obtain different values of dynamic Stokes number. With $\rho_p/\rho_f \in [200, 20\,000]$, it leads to a range of dynamic Stokes number from 0.073 to 6.39. Since particle diameter is smaller than the Kolmogorov scale, particles are numerically treated under the point-particle approximation. As such, the particle charge Q_p is considered to be concentrated at one point (particle's centre of mass) defined as $Q_p = \pi d_p^2 \rho_Q$, where ρ_Q is the particle surface charge density. It should be noted here, that according to Hamamoto, Nakajima & Sato (1992) there is a saturation limit of surface charge density for small spheres, which can be translated (via d_p) to a corresponding limit for point-particle charges.

For the configuration presented in this work, this value can be estimated to be approximately 4 nC. The various particle charges, that have been considered, are all given in terms of a reference charge $Q_0 = 1$ nC (Boutsikakis *et al.* 2020) which is of the same order of magnitude as the aforementioned limit. To explore the effect of electrostatic forces through the electrostatic Stokes number, particle charge varies from $0.1Q_0$ to $10Q_0$ which leads to an electrostatic Stokes variation in the range of 3×10^{-3} to 2.8. Figure 2 shows all dynamic and electrostatic Stokes numbers investigated in the present paper.

3. Effect of electrostatic forces on the dispersion of charged particles

In this section we first examine how the particle dispersion coefficient is affected by electrostatic forces. The dispersion of solid particles transported by a turbulent flow has been extensively investigated, for example, by Tchen (1947), Hinze (1972), Gouesbet, Berlemont & Picart (1982, 1984), Deutsch & Simonin (1991), Simonin, Deutsch & Minier (1993) and Pascal & Oesterlé (2000). Mathematically, the dispersion coefficient, D^t_p, is related to the variance of particle displacement. Hence, it is defined as

$$D^t_p = \lim_{\tau \rightarrow +\infty} \frac{1}{6}\frac{\mathrm{d}}{\mathrm{d}\tau}\langle (\boldsymbol{x}_p(t + \tau) - \boldsymbol{x}_p(t))^2 \rangle_p. \tag{3.1}$$

Figure 3 shows the time evolution of the particle displacement variance measured in DNS. After a transitory phase, the variance of displacement has a linear evolution. To compute the dispersion coefficient over long times, a linear regression is performed for the last 45 % of the temporal signal (after the vertical line on figure 3) and the slope corresponds to the dispersion coefficient.

As a classic result, the time for reaching the established dispersion depends on the particle relaxation time scale. The smaller the relaxation time scale, the shorter the
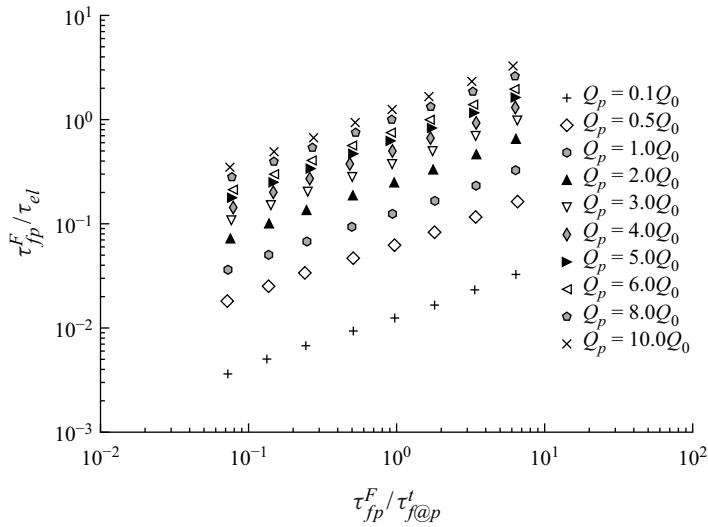
Figure 2. Dynamic ($\tau_{fp}^F/\tau_{f@p}^t$) and electrostatic Stokes (τ_{fp}^F/τ_{el}) numbers of the numerical simulations used in the study. Each point corresponds to a case differing by the dynamic Stokes number or by the electrostatic Stokes number.
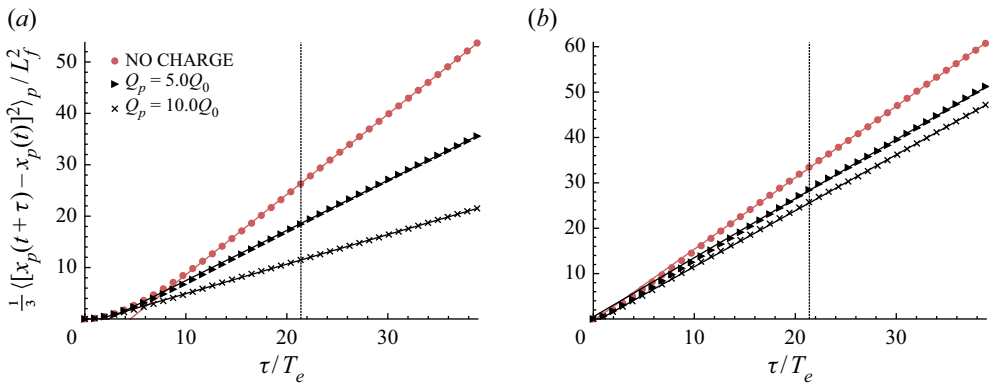

Figure 3. Time-evolution of the mean square displacement of particles for $\tau_{fp}^F/\tau_{f@p}^t = 6.39$ (*a*) and $\tau_{fp}^F/\tau_{f@p}^t = 0.073$ (*b*). Symbols represent the data from DNS, while solid lines the linear regression performed on the data at long times, namely after the vertical lines. Plot (*a*) shows electrostatic Stokes numbers $\tau_{fp}^F/\tau_{el} = 1.63$ ($Q_p = 5.0Q_0$) and $\tau_{fp}^F/\tau_{el} = 3.27$ ($Q_p = 10.0Q_0$). Plot (*b*) shows electrostatic Stokes numbers $\tau_{fp}^F/\tau_{el} = 0.18$ ($Q_p = 5.0Q_0$) and $\tau_{fp}^F/\tau_{el} = 0.35$ ($Q_p = 10.0Q_0$).

transient period. Concerning the effect of the electric charge, one observes that particle dispersion decreases with increasing the charge.

Figure 4 shows the particle dispersion coefficient normalized by the value in the charge-free case with respect to both the dynamic and electrostatic Stokes numbers. We first observe that for a small electrostatic Stokes number (i.e. $\tau_{fp}^F/\tau_{el} < 0.1$), there is no effect of the charges on the particle dispersion coefficient. In contrast, for $\tau_{fp}^F/\tau_{el} > 0.1$, the dispersion coefficient decreases with increasing the electrostatic Stokes number. That trend is observed for all dynamic Stokes numbers, and it can be noticed that for the smallest Stokes number $\tau_{fp}^F/\tau_{f@p}^t = 0.073$, the modification by inter-particle electrostatic forces is
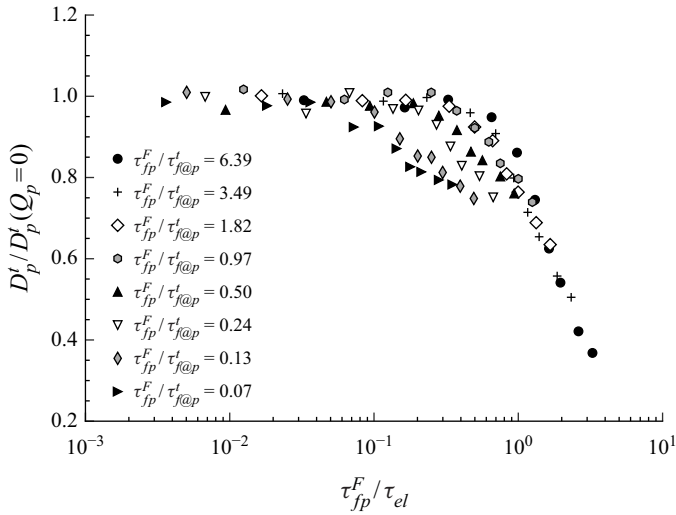
Figure 4. Effect of the charge on the particle dispersion coefficient with respect to the dynamic Stokes number and the electrostatic Stokes number.

smaller than for the particles with the highest Stokes number $\tau_{fp}^F/\tau_{f@p}^t = 6.39$. For the latter, the decrease of particle dispersion is up to 60 %.

In homogeneous isotropic turbulent flows the dispersion coefficient may also by computed with the expression (Hinze 1972)

$$D_p^t = \tfrac{2}{3} q_p^2 \tau_p^t, \tag{3.2}$$

where we remind that $q_p^2 = 1/2 \langle u_{p,i}' u_{p,i}' \rangle_p$ is the particle kinetic energy (per unit mass) and $\tau_p^t = \int_0^{+\infty} R_p(\tau)\,\mathrm{d}\tau$ is the Lagrangian particle integral time scale with the particle velocity auto-correlation function, R_p, defined by (2.8).

Figure 5 shows that for all charges and all particle inertia, the deviation between the measured particle dispersion coefficient and the Tchen–Hinze theoretical model (3.2) is less than 5 %. It means that even if the particle dispersion coefficient is modified by the inter-particle electrostatic forces, the relation between the dispersion coefficient to the particle agitation and the Lagrangian particle integral time scale remains unchanged. From this, in the following sections we scrutinize how the particle agitation and the particle velocity auto-correlation time scale are both modified by the electrostatic forces.

4. Modification of particle kinetic energy and fluid–particle velocity covariance by electrostatic forces

The modulation of particle kinetic energy by electrostatic forces is shown by Figure 6. As expected, for small values of the electrostatic Stokes number, the particle agitation is found unchanged by the electrostatic forces. For $\tau_{fp}^F/\tau_{el} > 5 \times 10^{-2}$, non-monotonic modifications of the particle agitation are observed. As, for example, considering the case of $\tau_{fp}^F/\tau_{f@p}^t = 0.13$ for an increasing electrostatic Stokes number, the particle agitation increases first and then decreases for large values of the electrostatic Stokes number. The same behaviour is also observed for larger values of the dynamic Stokes number.

Such evolution could be surprising because the inter-particle electrostatic forces are conservative and should not modify the particle kinetic energy. However, as shown by
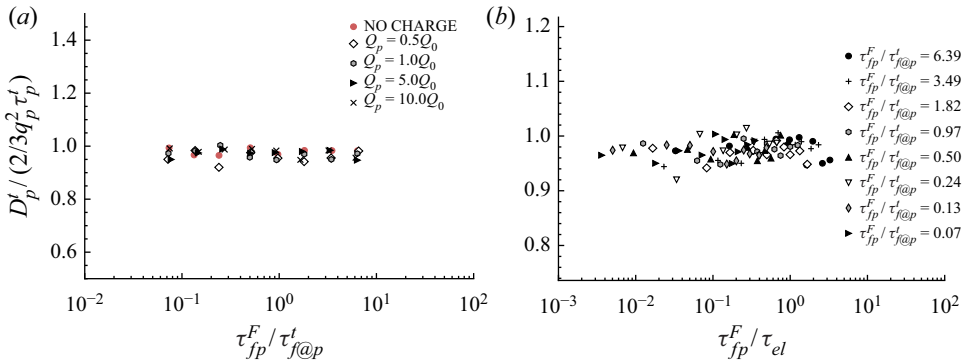
Figure 5. Measured particle dispersion coefficient normalized by the model standard expression (3.2) with respect to dynamic (*a*) and electrostatic Stokes numbers (*b*).
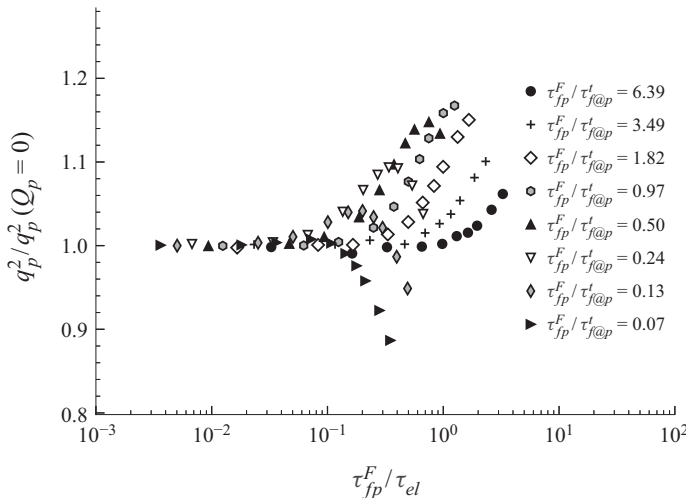

Figure 6. Effect of the electrostatic charges on the particle kinetic energy with respect to the dynamic Stokes number and to the electrostatic Stokes number.

Boutsikakis *et al.* (2020), the modulation of the particle kinetic energy by the electrostatic forces is, in fact, an indirect effect due to the modification of the fluid–particle covariance $q_{fp} = \langle u'_{p,i} u'_{f@p,i} \rangle_p$ by electrostatic forces. Indeed, following the Tchen–Hinze theory, the particle kinetic energy is related to the fluid–particle velocity covariance by Tchen (1947) (see also Hinze 1972 or Gouesbet *et al.* 1984) as

$$2q_p^2 = q_{fp}. \tag{4.1}$$

Figure 7 shows (4.1) with respect to the electrostatic Stokes number. One can observe that, for the wide range of investigated electrostatic Stokes numbers, the relation (4.1) is always satisfied. In the present case, figure 6 shows a maximum modification of the particle kinetic energy on the order of 20 % that can not explain, just by itself, the modification of the particle dispersion coefficient (see figure 4).

In the framework of the joint probability density function (PDF) approach (see Zaichik, Simonin & Alipchenkov 2003, 2006; Reeks, Simonin & Fede 2016 for details), it is possible to derive the following transport equation for the fluid–particle velocity
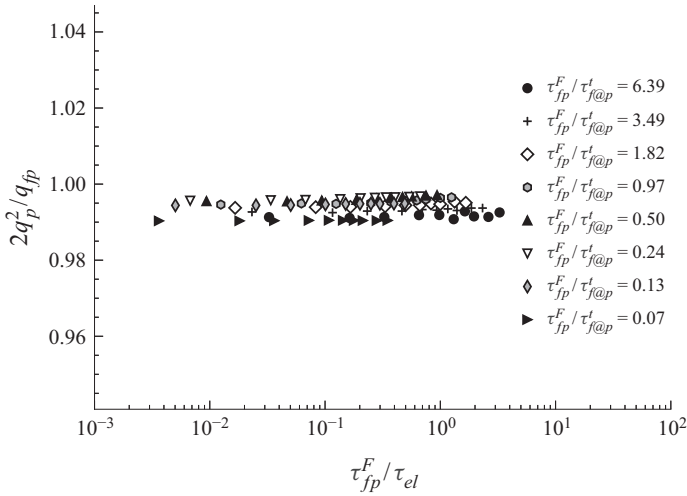
Figure 7. Effect of the electrostatic charges on the Tchen–Hinze equilibrium defined by (4.1).

covariance (Deutsch & Simonin 1991; Simonin 1996):

$$\frac{\mathrm{d}q_{fp}}{\mathrm{d}t} = \left\langle \frac{\boldsymbol{F}_d}{m_p} \boldsymbol{u}'_{f@p} \right\rangle_p + \langle \boldsymbol{a}'_{f@p} \boldsymbol{u}'_p \rangle_p + \left\langle \frac{\boldsymbol{F}_e}{m_p} \boldsymbol{u}'_{f@p} \right\rangle_p . \qquad (4.2)$$

Here $\boldsymbol{a}_{f@p} = \mathrm{d}\boldsymbol{u}_{f@p}/\mathrm{d}t$ is the acceleration of the fluid seen by the particles. In (4.2) the first term on the right-hand-side is the effect of the entrainment by fluid turbulence due to drag force on the fluid–particle covariance. With (2.5) this term reads as

$$\left\langle \frac{\boldsymbol{F}_d}{m_p} \boldsymbol{u}'_{f@p} \right\rangle_p = -\frac{q_{fp} - 2q^2_{f@p}}{\tau^F_{fp}}, \qquad (4.3)$$

where two contributions appear: first, a dissipative term by the viscous friction of the particles with the fluid and, second, the transfer of kinetic energy from the turbulence towards the particles. The second term in (4.2) represents the correlation between the acceleration of the fluid seen by the particles and the particle fluctuating velocity. Figure 8 shows the evolution of this term with respect to the dynamic and electrostatic Stokes numbers. From the left panel it can be observed that, even without electric charge, this term depends on the dynamic Stokes number. The two asymptotic trends were expected because, on one hand, when particle inertia is large, the particle velocity is uncorrelated with the fluid velocity and acceleration, hence, $\langle \boldsymbol{a}'_{f@p} \boldsymbol{u}'_p \rangle_p \to 0$. On the other hand, when the particle relaxation time scale is very small hence $\langle \boldsymbol{a}'_{f@p} \boldsymbol{u}'_p \rangle_p \to \langle \boldsymbol{a}'_f \boldsymbol{u}'_f \rangle_f$ but in stationary homogeneous isotropic turbulent flow $\langle \boldsymbol{a}'_f \boldsymbol{u}'_f \rangle_f \to 0$. When the electrostatic Stokes number increases, figure 8 shows that $\langle \boldsymbol{a}'_{f@p} \boldsymbol{u}'_p \rangle_p$ is decreasing. As a direct conclusion, the electrostatic forces lead to a decrease of the correlation between the particle velocity and the local fluid acceleration. Furthermore, such a destruction of the fluid–particle velocity covariance is even larger for larger dynamic Stokes numbers.

Finally, the last term on the right-hand side of (4.2) is the effect of the electrostatic forces on the fluid–particle covariance. Figure 9 shows this term measured in the DNS with respect to the electrostatic Stokes number. Such a term is found negative, meaning that the electrostatic force destructs the fluid–particle covariance. As expected, this term increases
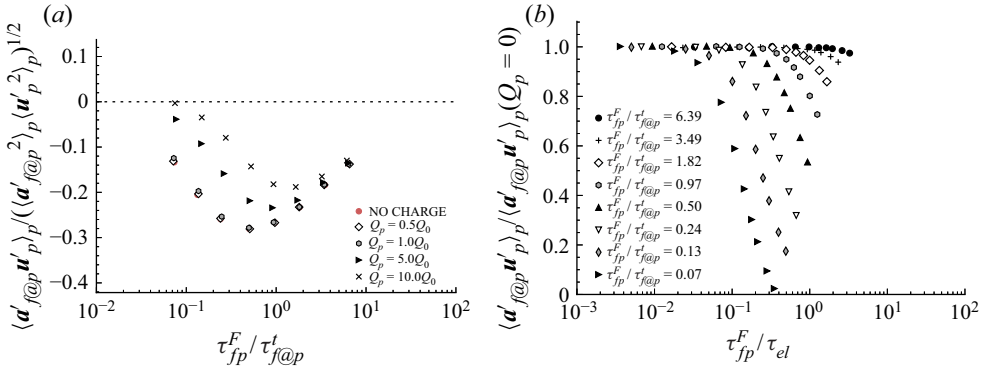
Figure 8. Fluid–particle interaction term with respect to the dynamic (*a*) and the electric (*b*) Stokes numbers.

when the electrostatic Stokes number increases. Figure 6 shows a non-monotonic evolution of the particle kinetic energy as a function of the electrostatic Stokes number which can be explained as follows. Indeed, considering the relevant case of $\tau_{fp}^F/\tau_{f@p}^t = 0.13$, when τ_{fp}^F/τ_{el} is larger than 5×10^{-2}, we observe an increase of q_p^2. This is explained by the fact that the electrostatic forces decrease the intensity of $\langle a'_{f@p} u'_p \rangle_p$, which is negative (see figure 8*a*). As a result, the fluid–particle velocity covariance increases and consequently does the particle kinetic energy. At that time, the direct destruction of the fluid–particle covariance by electrostatic forces also acts but its effect is weak. However, for approximately $\tau_{fp}^F/\tau_{el} > 2 \times 10^{-1}$, this direct destruction term dominates, leading to the decrease of the particle kinetic energy.

To model the effect of the electrostatic forces, it is possible to make an analogy with elastic inter-particle collisions. Fundamentally, the main difference is the collision distance, which is, for the latter, the particle diameter (i.e. two colliding particle have to be in contact). For the electrostatic force, collisions occur at a given effective distance larger than the particle diameter (note that in the literature dedicated to the plasma, the terminology 'Coulomb collisions' is used to denote electrostatic interactions). This analogy leads to two consequences. First, the inter-particle collision time scale τ_{col}, which is the time for one particle to have a collision with any other particle, may be substituted by the characteristic time scale of electrostatic forces τ_{el}. Second, the electrostatic effect in the PDF approach can be treated as a collision with a frequency $1/\tau_{el}$ and occurring at the effective distance d_{el}. This last parameter can be estimated from works done in plasma where they estimate the Coulomb collision cross-section by

$$d_{el} = \frac{1}{2\pi\epsilon_0} \frac{Q_p^2}{m_p \langle ||w_r|| \rangle_p^2}, \tag{4.4}$$

where w_r is the inter-particle relative velocity that is given by $\langle ||w_r|| \rangle_p = \sqrt{32q_p^2/(3\pi)}$. The analogy between inter-particle collisions and Coulomb collisions allows us to explain why the fluid–particle covariance decreases with the electrostatic forces, and also to model this said destruction. First, in case of elastic inter-particle collisions, Laviéville *et al.* (1997) and later Fede, Simonin & Villedieu (2015) explained that if particles are smaller than the smallest turbulent scale (i.e. the Kolmogorov length scale), two colliding particles see nearly the same velocity. As a matter of fact, the fluid–particle covariance of the two

938 A33-12

colliding particles is conserved because of the conservation of momentum (reminder that only elastic collisions are considered).

To explain a pathological non-physical destruction of the fluid–particle covariance, observed in the Lagrangian stochastic approach, Laviéville *et al.* (1997) (see also Sommerfeld 2001; Fede *et al.* 2015; Fede & Simonin 2018) derived analytically the fluid–particle destruction term at a given distance. Replacing the collision time scale with the electric one, it is written as

$$\left\langle \frac{F_e}{m_p} u_{f@p} \right\rangle_p = -\frac{2}{3}[1 - f(d_{el})]\frac{q_{fp}}{\tau_{el}}, \tag{4.5}$$

where $f(r)$ is the fluid velocity spatial auto-correlation function, with the asymptotic behaviours $f(r = 0) = 1$ (more precisely it is for $r < \eta_K$) and for large distances $\lim_{r \to +\infty} f(r) = 0$. In first approximation, such a function can be approximated using an exponential function

$$f(r) = \exp\left[-\frac{r}{L_f}\right], \tag{4.6}$$

but, for short distances, a two-exponential model can be used,

$$f(r) = \frac{\exp\left[-\frac{\chi^2 r}{L}\right] - \chi^2 \exp\left[-\frac{r}{L}\right]}{1 - \chi^2}, \tag{4.7}$$

where χ and L are the solutions of $L = L_f(1 + 1/\chi^2)^{-1}$ and $\chi = L/\lambda_g$. A similar two-scale model has also been proposed by Sawford (1991) for the fluid velocity Lagrangian auto-correlation function. The choice of the model may lead to differences in the predictions of the fluid–particle velocity covariance destruction by (4.5). Figure 10 shows the relative position of the Coulomb collision diameter d_{el} to the Eulerian integral length scale, L_f, with respect to both models and also with regards to the dynamic Stokes number.

Figure 9 shows the comparison between $\langle F_e u_{f@p} \rangle_p / m_p$ measured in DNS and the predictions given by (4.5). The dashed lines correspond to the original model proposed by Laviéville *et al.* (1997) corresponding to $d_{el} \gg L_f$, hence, $f(d_{el}) = 0$. The solid lines are the prediction with (4.7) and (4.4). Two main conclusions can be drawn from figure 9. First, the electrostatic term is negative, hence, it is really a destruction term of the fluid–particle velocity covariance. Second, the model predictions are in agreement with the DNS data.

5. Effect of electrostatic forces on the particle velocity auto-correlation

To investigate the effect of the electrostatic forces on the Lagrangian particle integral time scale, one can start first by the particle velocity auto-correlation function. These correlation functions are given by figure 11. As expected, when the electric charge is increasing, the auto-correlation function decreases because the electrostatic forces decorrelate the particle velocities. Such an effect is found to be more important for a large dynamic Stokes number (left panel). As a direct consequence, the integral of the auto-correlation functions decrease for increasing particle charge. The decrease of the Lagrangian particle integral time scale with the dynamic Stokes number is shown by figure 12. Such a figure also shows a standard result, which is the increase of the Lagrangian particle integral time scale for increasing Stokes number (i.e. the larger the particle inertia, the longer the particle velocity is correlated with itself).
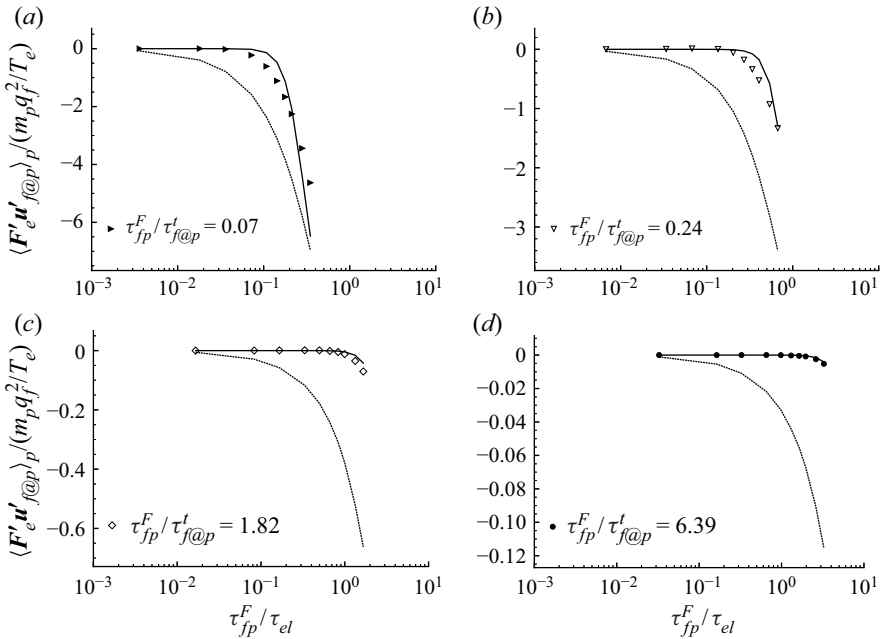
Figure 9. Electrostatic effect term in fluid–particle covariance with respect to the electrostatic Stokes number. Symbols represent the terms measured in DNS, while lines the predictions given by (4.5) with $f(r) = 0$ (dashed lines) and with $f(d_{el})$ given by (4.7) and (4.4) (solid lines).
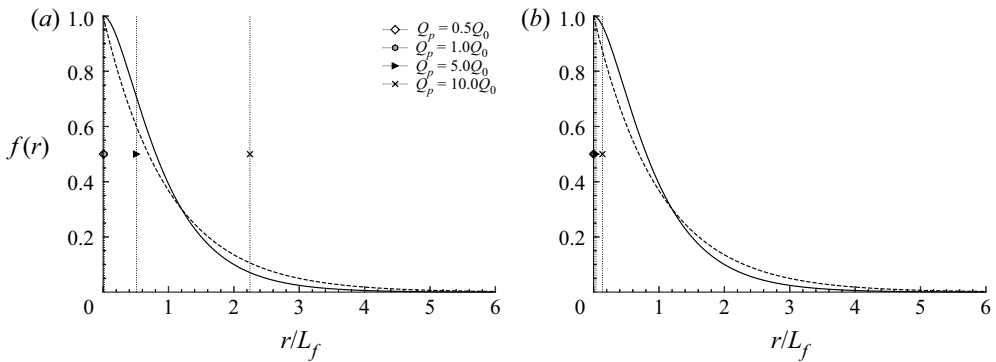

Figure 10. Spatial auto-correlation given by a single exponential function (4.6) (dashed line) and by a double-exponential function (4.7) (solid line) for $\tau_{fp}^F/\tau_{f@p}^t = 0.073$ (a) and $\tau_{fp}^F/\tau_{f@p}^t = 6.39$ (b). The vertical lines correspond to the value of d_{el}/L_f.

For the modelling of particle dispersion, a model is needed for the integral of the particle velocity auto-correlation function, namely the Lagrangian particle integral time scale τ_p^t, but also for the shape of the auto-correlation function. To show how the electrostatic forces modify the shape of the auto-correlation function, figure 13 shows these functions with respect to the time normalized by the Lagrangian particle integral time scale. For a small dynamic Stokes number, the electrostatic forces have no effect on the shape of $R_p(\tau)$, and for a larger Stokes number, we observe that the particle velocity auto-correlation function tends to an exponential function. These differences occur essentially for a short time $\tau \to 0$.
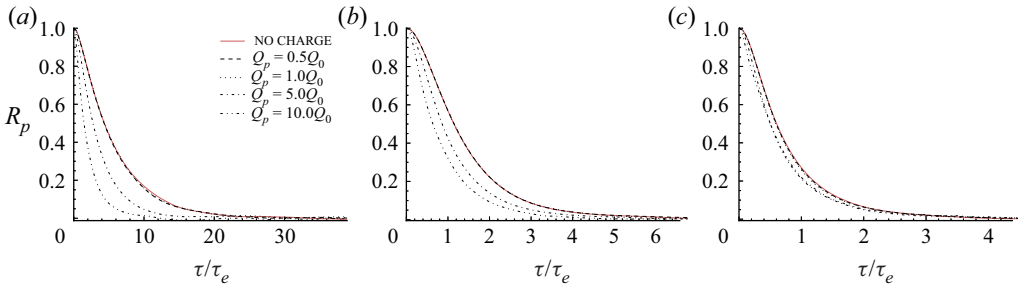
938 A33-14

Figure 11. Effect of the electrostatic charges on the particle velocity auto-correlation function for $\tau_{fp}^F/\tau_{f@p}^t = 6.39$ (*a*), $\tau_{fp}^F/\tau_{f@p}^t = 0.97$ (*b*) and $\tau_{fp}^F/\tau_{f@p}^t = 0.073$ (*c*).
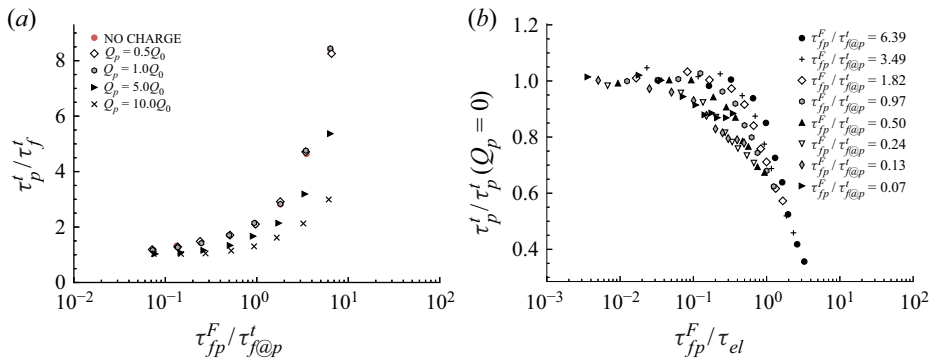

Figure 12. Lagrangian particle integral time scale normalized by the Lagrangian fluid integral time scale with respect to the dynamic Stokes number.
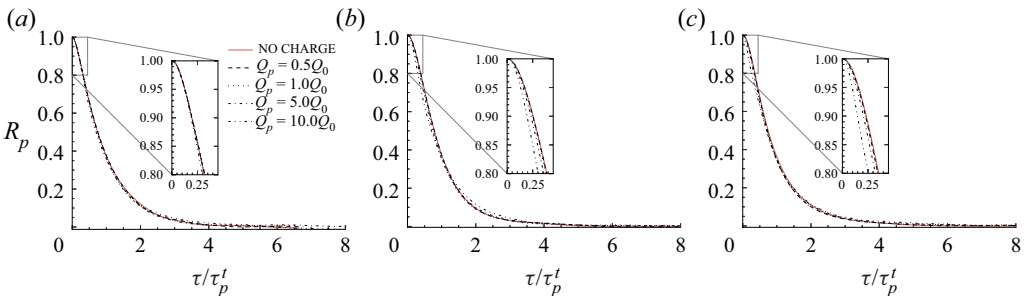

Figure 13. Effect of the electrostatic charges on the shape of the particle velocity Lagrangian auto-correlation function for $\tau_{fp}^F/\tau_{f@p}^t = 6.39$ (*a*), $\tau_{fp}^F/\tau_{f@p}^t = 0.97$ (*b*) and $\tau_{fp}^F/\tau_{f@p}^t = 0.073$ (*c*).

Laviéville, Deutsch & Simonin (1995) analysed the effect of inter-particle collisions on the dispersion of particles transported by homogeneous isotropic turbulence. The authors derived theoretically the expressions of the particle velocity auto-correlation function, Lagrangian particle integral time scale and particle dispersion coefficient taking into account the effect of the collisions. Making an analogy between particle collisions and Coulomb collisions, the particle velocity auto-correlation function proposed by
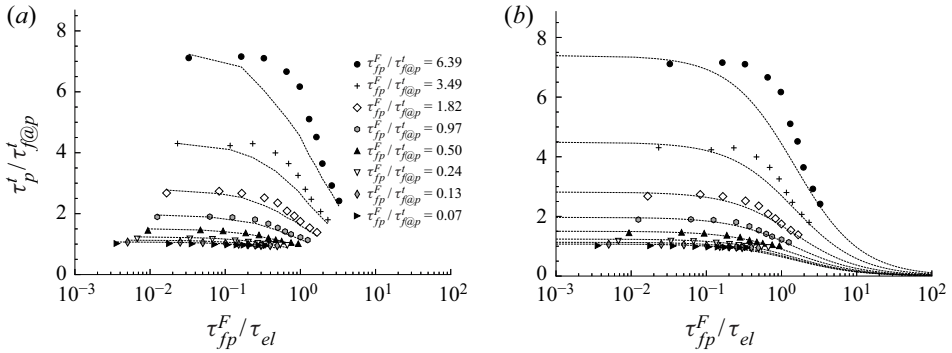
Figure 14. Lagrangian particle integral time scale with respect to the electrostatic Stokes number. Symbols represent the statistics from DNS, while lines the prediction of (5.2). (*a*) The model is computed with the DNS data (*a priori* test). (*b*) The model is computed with the data of the charge-free case.

Laviéville *et al.* (1995) can be rewritten as

$$R_p(\tau) = \exp\left(-\frac{\tau}{\tau_b}\right) + \frac{\tau_{f@p}^t \tau_b}{\tau_{fp}^F} \frac{\exp\left(-\dfrac{\tau}{\tau_b}\right) - \exp\left(-\dfrac{\tau}{\tau_{f@p}^t}\right)}{\tau_b - \tau_{f@p}^t}, \tag{5.1}$$

where $\tau_b = \tau_{fp}^F[1 + \frac{2}{3}(\tau_{fp}^F/\tau_{el})]^{-1}$. This model is based on two time scales, which is strictly equivalent to saying it is a two-exponential model. As shown by Deutsch & Simonin (1991), in case of no collisions ($\tau_{fp}^F/\tau_{el} \to 0$), the question of the one- or two-exponential model depends on the dynamic Stokes number. For a small Stokes number and/or fluid elements, the slope at the origin depends on the Reynolds number. A one-exponential model is more suitable for a high Reynolds number, and a two-exponential one is more adapted to a low Reynolds number (Sawford 1991). For moderate and large Stokes numbers, particle inertia leads the particle velocity to be correlated over a short time giving a non-zero slope of the auto-correlation function. Such an effect can be taken into account by the original model proposed by Laviéville *et al.* (1995). If the characteristic time scale of these mechanisms is smaller than the particle relaxation time scale, they asymptotically tend towards the single-exponential function.

The Lagrangian particle integral time scale with respect to the electrostatic Stokes number is shown by figure 14. As expected, the decorrelating effect of the electrostatic forces leads to the decreasing of the Lagrangian particle integral time scale. The magnitude of such a decrease explains why the particle dispersion coefficient decreases so strongly when the electrostatic Stokes number increases (see figure 4). From the auto-correlation function (5.1), Laviéville *et al.* (1995) derived theoretically the evolution of the Lagrangian particle integral time scale as a function of the inter-particle collision time scale. Replacing such a time scale by the characteristic one of the electrostatic forces leads to the following expression:

$$\frac{\tau_p^t}{\tau_{f@p}^t} = \left[1 + \frac{\tau_{fp}^F}{\tau_{f@p}^t}\right] \times \left[1 + \frac{2}{3}\frac{\tau_{fp}^F}{\tau_{el}}\right]^{-1}. \tag{5.2}$$

Figure 14 compares the prediction of (5.2) with our DNS data. The left panel is an *a priori* test, in the sense that the model predictions are computed with our DNS data. It has to be
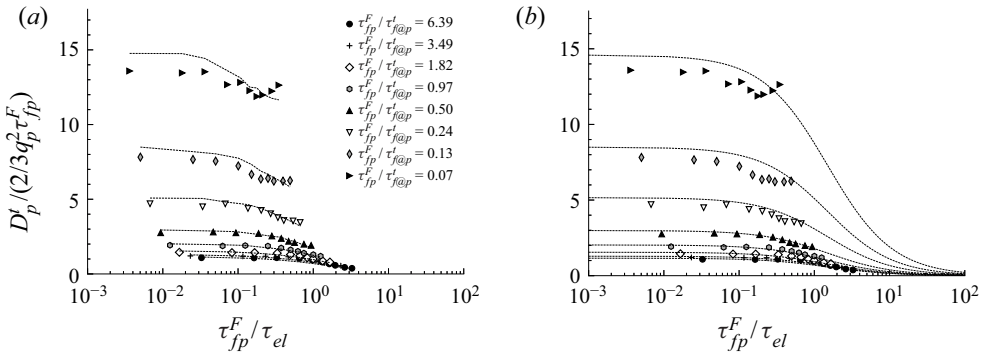
938 A33-16

Figure 15. Particle dispersion coefficient with respect to the electrostatic Stokes number. Symbols represent the statistics from DNS, while lines the prediction of (5.3). (*a*) The model is computed using the data from DNS (*a priori* test). (*b*) The model is computed with the data of the charge-free case.

contrasted with the right panel where $\tau^t_{f@p}$ and τ^F_{fp} of the charge-free cases have been used for computing the model predictions. Figure 14 shows a good agreement between the DNS and the model predictions.

The last step of this study consists of the prediction of the particle dispersion coefficient modulation by electrostatic forces. As previously stated, we propose drawing an analogy between the inter-particle and Coulomb collisions. Following the model proposed by Laviéville *et al.* (1995), the particle dispersion coefficient can be predicted by

$$D^t_p = \frac{2}{3} q^2_p \tau^F_{fp} \left[1 + \frac{\tau^t_{f@p}}{\tau^F_{fp}} \right] \times \left[1 + \frac{2}{3} \frac{\tau^F_{fp}}{\tau_{el}} \right]^{-1}. \tag{5.3}$$

Figure 15 shows the comparison between DNS data and predictions given by (5.3). As for figure 14, the left panel shows model predictions that have been computed with the DNS data and the right panel with the data from the charge-free cases. A very good agreement is observed between the model and the DNS data.

6. Conclusions

The paper analyses the effects of electrostatic forces on the dispersion of like-charged inertial particles transported by homogeneous isotropic turbulent flows. Direct numerical simulation coupled with Lagrangian tracking of charged particles have been performed, where the particle motion is controlled only by the drag and electrostatic forces. According to the very low solid volume fraction considered, both two-way coupling and inter-particle collisions are neglected.

The numerical simulations show that the particle dispersion coefficient decreases when the electrostatic Stokes number is increasing. Since the dispersion of particles by turbulent flow is related to the particle agitation intensity and also to the Lagrangian integral time scale of the particle velocities, these two quantities have been analysed with respect to the dynamic and electrostatic Stokes numbers.

As already shown by Boutsikakis *et al.* (2020), particle agitation decreases with increasing electrostatic Stokes number. However, the local equilibrium between the particle agitation and the fluid–particle covariance is still satisfied, namely $2q^2_p = q_{fp}$. Hence, the destruction of particle agitation by electrostatic forces is an indirect effect, because it comes from the destruction of the fluid–particle covariance q_{fp}.

938 A33-17

When analysing the transport equation of the latter, we show that the electrostatic forces have two effects. First, they decrease the correlation between the fluid acceleration and the particle velocity (indirect effect). Second, the electrostatic forces act as a destruction term of the fluid–particle covariance (direct effect). The non-monotonic evolution of the particle kinetic energy results from the competition of these two effects. Treating electrostatic interactions as Coulomb collisions, the model proposed by Laviéville *et al.* (1995), for predicting the fluid–particle covariance destruction by inter-particle collisions, has been compared with the DNS results. We show that if the collision time scale is replaced by the electrostatic time scale, it is possible to predict the destruction of the fluid–particle covariance. As expected, the Lagrangian particle integral time scale is found decreasing when increasing the electrostatic Stokes number because of the decorrelating nature of the (repulsive) electrostatic forces. Again, we show that the predictions of the model proposed by Laviéville *et al.* (1995) are in agreement with the DNS.

From a modelling point of view, we show that the models proposed for inter-particle collisions can be used for predicting the like-charged particle dispersion in turbulent flows. However, these models assume that the spatial distribution of the particles is uniform, i.e. no preferential concentration. Moreover, it has been shown by Lu *et al.* (2010*a*) that electrostatic forces may modify the spatial particle distribution through the modification of the radial distribution function.

Author ORCIDs.

Ⓓ Athanasios Boutsikakis https://orcid.org/0000-0001-6083-3838;

Ⓓ Pascal Fede https://orcid.org/0000-0002-0368-4829;

Ⓓ Olivier Simonin https://orcid.org/0000-0002-2794-7662.

REFERENCES

ALIPCHENKOV, V.M., ZAICHIK, L.I. & PETROV, O.F. 2004 Clustering of charged particles in isotropic turbulence. *High Temp.* **42** (6), 919–927.

BOUTSIKAKIS, A., FEDE, P., PEDRONO, A. & SIMONIN, O. 2020 Numerical simulations of short- and long-range interaction forces in turbulent particle-laden gas flows. *Flow Turbul. Combust.* **105** (4), 989–1015.

DEUTSCH, E. & SIMONIN, O. 1991 Large eddy simulation applied to the motion of particles in stationary homogeneous fluid turbulence. *Proc. ASME-FED* **110**, 35–42.

ESWARAN, V. & POPE, S.B. 1988 An examination of forcing in direct numerical simulations of turbulence. *Comput. Fluids* **16**, 257–278.

FEDE, P. & SIMONIN, O. 2006 Numerical study of the subgrid fluid turbulence effects on the statistics of heavy colliding particles. *Phys. Fluids* **18**, 045103.

FEDE, P. & SIMONIN, O. 2018 Direct simulation Monte-Carlo predictions of coarse elastic particle statistics in fully developed turbulent channel flows: comparison with deterministic discrete particle simulation results and moment closure assumptions. *Intl J. Multiphase Flow* **108**, 25–41.

FEDE, P., SIMONIN, O. & VILLEDIEU, P. 2015 Monte-Carlo simulation of colliding particles or coalescing droplets transported by a turbulent flow in the framework of a joint fluid–particle pdf approach. *Intl J. Multiphase Flow* **74** (0), 165–183.

FESSLER, J.R., KULICK, J.D. & EATON, J.K. 1994 Preferential concentration of heavy particles in a turbulent channel flow. *Phys. Fluids* **6**, 3742–3749.

FÉVRIER, P., SIMONIN, O. & SQUIRES, K.D. 2005 Partitioning of particle velocities in gas-solid turbulent flows into a continuous field and a spatially uncorrelated random distribution: theoretical formalism and numerical study. *J. Fluid Mech.* **533**, 1–46.

GATIGNOL, R. 1983 The Faxen formulae for a rigid particle in an unsteady non uniform Stokes flow. *J. Méc.* **9**, 143–160.

GOUESBET, G., BERLEMONT, A. & PICART, A. 1982 On the Tchen's theory of discrete particles dispersion: can dense discrete particles disperse faster than fluid particles? *Lett. Heat Mass Transfer* **9** (5), 407–419.

GOUESBET, G., BERLEMONT, A. & PICART, A. 1984 Dispersion of discrete particles by continuous turbulent motions. Extensive discussion of the Tchen's theory, using a two-parameter family of Lagrangian correlation functions. *Phys. Fluids* **27** (4), 827837.

GROSSHANS, H., BISSINGER, C., CALERO, M. & PAPALEXANDRIS, M.V. 2021 The effect of electrostatic charges on particle-laden duct flows. *J. Fluid Mech.* **909**, A21.

HAMAMOTO, N., NAKAJIMA, Y. & SATO, T. 1992 Experimental discussion on maximum surface charge density of fine particles sustainable in normal atmosphere. *J. Electrostat.* **28** (2), 161–173.

HINZE, J.O. 1972 Turbulent fluid and particle interaction. *Prog. Heat Mass Transfer* **6**, 433–452.

KARNIK, A.U. & SHRIMPTON, J.S. 2012 Mitigation of preferential concentration of small inertial particles in stationary isotropic turbulence using electrical and gravitational body forces. *Phys. Fluids* **24** (7), 073301.

LAVIÉVILLE, J., DEUTSCH, E. & SIMONIN, O. 1995 Large eddy simulation of interaction between colliding particles and a homogeneous isotropic turbulence field. *ASME-Publications-Fed* **228**, 347–358.

LAVIÉVILLE, J., SIMONIN, O., BERLEMONT, A. & CHANG, Z. 1997 Validation of inter-particle collision models based on Large Eddy Simulation in gas-solid turbulent homogeneous shear flow. In *Proceedings of the 7th International Symposium on Gas-Particle Flows ASME FEDSM97-3623*.

LI, A. & AHMADI, G. 1993 Aerosol particle deposition with electrostatic attraction in a turbulent channel flow. *J. Colloid Interface Sci.* **158** (2), 476–482.

LU, J., NORDSIEK, H., SAW, E.W. & SHAW, R.A. 2010*a* Clustering of charged inertial particles in turbulence. *Phys. Rev. Lett.* **104**, 184505.

LU, J., NORDSIEK, H. & SHAW, R.A. 2010*b* Clustering of settling charged particles in turbulence: theory and experiments. *New J. Phys.* **12** (12), 123030.

LU, J. & SHAW, R.A. 2015 Charged particle dynamics in turbulence: theory and direct numerical simulations. *Phys. Fluids* **27** (6), 065111.

MAXEY, M.R. & RILEY, J.J. 1983 Equation of motion for a small rigid sphere in a non uniform flow. *Phys. Fluids* **26** (4), 2883–2889.

MONIN, A.S. & YAGLOM, A.M. 2007 *Statistical Fluid Mechanics*, vol. 1. Dover.

PARKER, K.R. 1997 Why an electrostatic precipitator? In *Applied Electrostatic Precipitation*, pp. 1–10. Springer.

PASCAL, P.. & OESTERLÉ, B. 2000 On the dispersion of discrete particles moving in a turbulent shear flow. *Intl J. Multiphase Flow* **26**, 293–325.

PRUPPACHER, H.R. & KLETT, J.D. 2010 *Microphysics of Clouds and Precipitation*. Springer.

REEKS, M., SIMONIN, O. & FEDE, P. 2016 PDF models for particle transport, mixing and collisions in turbulent gas flows. In *Multiphase Flow Handbook*, 2nd edn (ed. E.E. Michaelides, C.T. Crowe & J.D. Schwarzkopf), pp. 144–202. CRC.

SAWFORD, B.L. 1991 Reynolds number effects in Lagrangian stochastic models of turbulent dispersion. *Phys. Fluids* **3** (6), 1577–1586.

SCHILLER, L. & NAUMANN, A. 1935 A drag coefficient correlation. *VDI Zeitung* **77**, 318–320.

SIMONIN, O. 1996 Combustion and turbulence in two-phase flows. In *Lecture Series 1996-02*. Von Kármán Institute for Fluid Dynamics.

SIMONIN, O., DEUTSCH, E. & MINIER, J.P. 1993 Eulerian prediction of the fluid/particle correlated motion in turbulent two-phase flows. *Appl. Sci. Res.* **51**, 275–283.

SOMMERFELD, M. 2001 Validation of a stochastic lagrangian modelling approach for inter-particle collisions in homogeneous isotropic turbulence. *Intl J. Multiphase Flow* **27**, 1829–1858.

TCHEN, C.M. 1947 Mean value and correlation problems connected with the motion of small particles suspended in a turbulent fluid. PhD thesis, Delft, Martinus Nijhoff, The Hague.

YAO, Y. & CAPECELATRO, J. 2018 Competition between drag and Coulomb interactions in turbulent particle-laden flows using a coupled-fluid–Ewald-summation based approach. *Phys. Rev. Fluids* **3**, 034301.

ZAICHIK, L.I., SIMONIN, O. & ALIPCHENKOV, V.M. 2003 Two statistical models for predicting collision rates of inertial particles in homogeneous isotropic turbulence. *Phys. Fluids* **15**, 2995–3005.

ZAICHIK, L.I., SIMONIN, O. & ALIPCHENKOV, V.M. 2006 Collision rates of bidisperse inertial particles in isotropic turbulence. *Phys. Fluids* **18** (3), 035110.